Journal of Mammalogy, XX(X):1–14, 2019
DOI:10.1093/jmammal/gyz087

Genetic variation and relationships among Afrotropical species of *Myotis* (Chiroptera: Vespertilionidae)

Bruce D. Patterson,* Paul W. Webala, Julian C. Kerbis Peterhans, Steven M. Goodman, Michael Bartonjo, and Terrence C. Demos

Integrative Research Center, Field Museum of Natural History, Chicago, IL 60605-2496, USA (BDP, JCKP, SMG, TCD)
Roosevelt University, 430 S. Michigan Ave, Chicago, IL 60605, USA (JCKP)
Department of Forestry and Wildlife Management, Maasai Mara University, P.O. Box 861-20500, Narok, Kenya (PWW)
Mammalogy Section, National Museums of Kenya, P.O. Box 40658-00100, Nairobi, Kenya (MB)

** Correspondent: bpatterson@fieldmuseum.org*

The genus *Myotis* is nearly cosmopolitan and the second-most speciose genus of mammals, but its Afrotropical members are few and poorly known. We analyzed phylogenetic and phylogeographic relationships of six of the eight known Afrotropical species using *Cytb* and sequences from four nuclear introns. Using Bayesian and maximum-likelihood approaches to generate single-locus, concatenated, and species trees, we confirmed prior evidence that the clade containing Afrotropical *Myotis* also contains both Palearctic and Indomalayan members. Additionally, we demonstrate that *M. bocagii* is sister to the Indian Ocean species *M. anjouanensis*, that this group is sister to *M. tricolor* and the Palearctic *M. emarginatus*, and find evidence suggesting that *M. welwitschii* is the earliest-diverging Afrotropical species and sister to the remainder. Although *M. tricolor* and *M. welwitschii* are both currently regarded as monotypic, both mitochondrial and nuclear data sets document significant, largely concordant geographic structure in each. Evidence for the distinction of two lineages within *M. tricolor* is particularly strong. On the other hand, geographic structure is lacking in *M. bocagii,* despite the current recognition of two subspecies in that species. Additional geographic sampling (especially at or near type localities), finer-scale sampling (especially in zones of sympatry), and integrative taxonomic assessments will be needed to better document this radiation and refine its nomenclature.

Key words: Afrotropical biodiversity, DNA sequence, East Africa, introgression, phylogeny, taxonomy

Mouse-eared bats, genus *Myotis*, are the only terrestrial mammals to attain a nearly cosmopolitan distribution independently of humans. In terms of species richness, *Myotis* (with 133 species) ranks second among living mammals only to the white-toothed shrews, *Crocidura* (with 198 species; mammaldiversity.org—Csorba et al. 2016). However, despite its huge range, the geographic diversification of *Myotis* has been decidedly uneven: 51 species occur in the Palearctic region, 31 in the Indomalayan region, 29 in the Neotropical region, 24 in the Nearctic region, 11 in Wallacea, and only eight in the Afrotropical region (mammaldiversity.org). In fact, two of the Afrotropical species are endemic to Madagascar and Anjouan Island (Comoros), respectively, so that sub-Saharan portions of the globe's second largest continent are home to only six species of *Myotis*. Does this reflect systematic undersampling of African biotas, or rampant but undetected cryptic speciation, or perhaps even competitive limitation and exclusion? Certainly, a number of other vespertilionid genera, including *Neoromicia* (18 species recognized), *Scotophilus* (at least 15 species), and *Pipistrellus* (13 species), are all more speciose in the Afrotropics than is *Myotis* (mammaldiversity.org—Demos et al. 2018).

The modest diversity of Afrotropical *Myotis* has attracted little systematic attention, and there has been no recent attempt to evaluate geographic variation of the six known continental species. The National Center for Biotechnology Information (GenBank) lacks any nucleotide sequences for two Afrotropical species, Ethiopian *M. morrisi* and Congolese *M. dieteri*, and has fewer than 50 total sequences of all loci for the other four continental species. By comparison, the same database hosts 1,149 nucleotide sequences for the European *Myotis myotis* and 78,405 for the North American *M. lucifugus*.

Early systematic analyses of the genus using mitochondrial DNA sequence analysis showed that the erstwhile subgenera of *Myotis* (*Myotis*, *Selysius*, and *Leuconoe*) represented convergently evolved ecomorphs rather than clades; each was found to be polyphyletic (Ruedi and Mayer 2001; see also Ghazali et al. 2017). A subsequent analysis that included the remaining subgenus, the endemic African *Cistugo*, confirmed its monophyly but placed it well outside *Myotis*; that analysis recovered the remaining African species (*M. welwitschii*, *M. bocagii*, *M. tricolor*, *M. goudoti*, and the Mediterranean *M. emarginatus*) as a well-supported African clade (Stadelmann et al. 2004). Bickham et al. (2004) also confirmed the clear distinction between *Myotis* and *Cistugo*, again based on *Cytb*; employing samples of additional species of Palearctic and Indomalayan *Myotis*, they recovered their lone Afrotropical species, *M. welwitschii*, as sister to Asian *M. formosus*, with that pair sister to *M. emarginatus.* A recent analysis by Ruedi et al. (2013) with superb taxonomic sampling (including 95 operational taxonomic units of *Myotis* sampled for *Cytb* and recombination activating gene, *Rag2*) confirmed the paraphyly of Afrotropical *Myotis*: two Asian taxa, *M. formosus* and *M. rufoniger* were included within the sampled African + Mediterranean grouping. In that recent analysis, each of the six Afrotropical taxa included was represented by a single pair of sequences (see also Ghazali et al. 2017).

Our recent systematic surveys of bats in East Africa and neighboring regions enable a closer examination of genetic variation among Afrotropical *Myotis*. Our goal was to assess population structure and species limits within this group and determine whether cryptic lineages were present. We used complete *Cytb* sequences and a set of four nuclear introns (1,759 bp) that have proven informative in studies of population structure and species delimitation involving other Afrotropical bat genera, including *Scotophilus* (Demos et al. 2018), *Rhinolophus* (Demos et al. In press-a), and *Nycteris* (Demos et al. In press-b). *Myotis* species in other regions are known to hybridize, and fuller genetic characterization is needed to understand whether mitochondrial introgression occurs among Afrotropical species. Despite well-differentiated nuclear gene pools, nearly a quarter of sampled *M. blythii* show mitochondrial introgression of *M. myotis* origin where these two European species overlap (Berthier et al. 2006). Genome-wide analyses show that despite mitochondrial introgression, the five currently recognized subspecies of *M. lucifugus* are paraphyletic, exchange alleles with other North American *Myotis* species in regions of contact, and warrant recognition as independent evolutionary lineages (Morales and Carstens 2018). The possibility of such discoveries for Afrotropical species of *Myotis* has been limited by poor sampling and reliance on mitochondrial sequences. Therefore, we sought to sequence both mitochondrial and nuclear loci from as many Afrotropical *Myotis* populations as possible, including finer-grained sampling in Kenya where the ranges of the three widespread Afrotropical species overlap. Our goal was to assess phylogeographic and phylogenetic relationships of Afrotropical *Myotis* and assess the potential evolutionary independence of any intraspecific lineages using independent nuclear and mitochondrial data sets.

Materials and Methods

Selection of taxa and sampling.—The majority of newly sequenced specimens in this study ($n = 50$) were from bats collected during field surveys using mist nets and harp traps placed in flyways or hand-held nets at roosts. Kenya was sampled especially broadly (Fig. 1). Initial species assignments were based on keys to the bats of East Africa (Patterson and Webala 2012). Field methods conformed to guidelines of the American Society of Mammalogists (Sikes et al. 2016) and were approved by the Field Museum of Natural History's IACUC (most recently 2012-003). The Kenya Wildlife Service (KWS/4001) and the Kenya Forest Service (RESEA/1/KFS/75) issued permits for Kenyan work. An additional 29 cytochrome-*b* (*Cytb*) sequences for *Myotis* were downloaded from GenBank. Two Afrotropical species, *M. anjouanensis* and *M. scotti*, were each represented by only a single sequence. Because of prior evidence for multiple Afrotropical-Asian colonization events, analyses included a variety of Asian and Palearctic species of *Myotis*, a member of the New World clade (*M. albescens*), a more distantly related vespertilionid (*Kerivoula argentata*), and a miniopterid (*Miniopterus aelleni*) to root relationships. In all, 78 individuals with 1–5 genes were analyzed for this study (see Appendix I for voucher numbers, locality data, and GenBank accession numbers).

Amplification, sequencing, and allele phasing.—Genomic DNA was extracted from tissue samples with the Wizard SV 96 Genomic DNA Purification System (Promega Corporation, Fitchburg, Wisconsin). Fresh specimens were sequenced for mitochondrial *Cytb*, using the primer pair LGL 765F and LGL 766R (Bickham et al. 1995; Bickham et al. 2004), and four unlinked autosomal nuclear introns: ACOX2 intron 3 (ACOX2), COPS7A intron 4 (COPS7A), and ROGDI intron 7 (ROGDI—Salicini et al. 2011); and STAT5A intron 16 (STAT5A—Eick et al. 2005). PCR amplifications were carried out using the same thermocycler protocols as in Demos et al. (2018). Amplified polymerase chain reaction (PCR) products were purified using ExoSAP-IT (Thermo Scientific, Waltham, Massachusetts). Sequencing was carried out in both directions on an ABI-3100 thermocycler (Applied Biosystems, Foster City, California) at the Pritzker Laboratory for Molecular Systematics and Evolution (FMNH).

Chromatographs were assembled and edited using GENEIOUS PRO v.11.1.5 (Biomatters Ltd., Auckland, New Zealand). Sequences from each locus were aligned independently using the MUSCLE algorithm (Edgar 2004) with default settings in GENEIOUS. Sequence data from *Cytb* were translated into amino acids and inspected for insertions, deletions, and internal stop codons to exclude paralogous sequences. Multiple gaps were included in the alignments of the nuclear introns, but their positions were unambiguous. Heterozygous nuclear intron alleles were statistically resolved using PHASE 2.1.1 (Stephens et al. 2001)

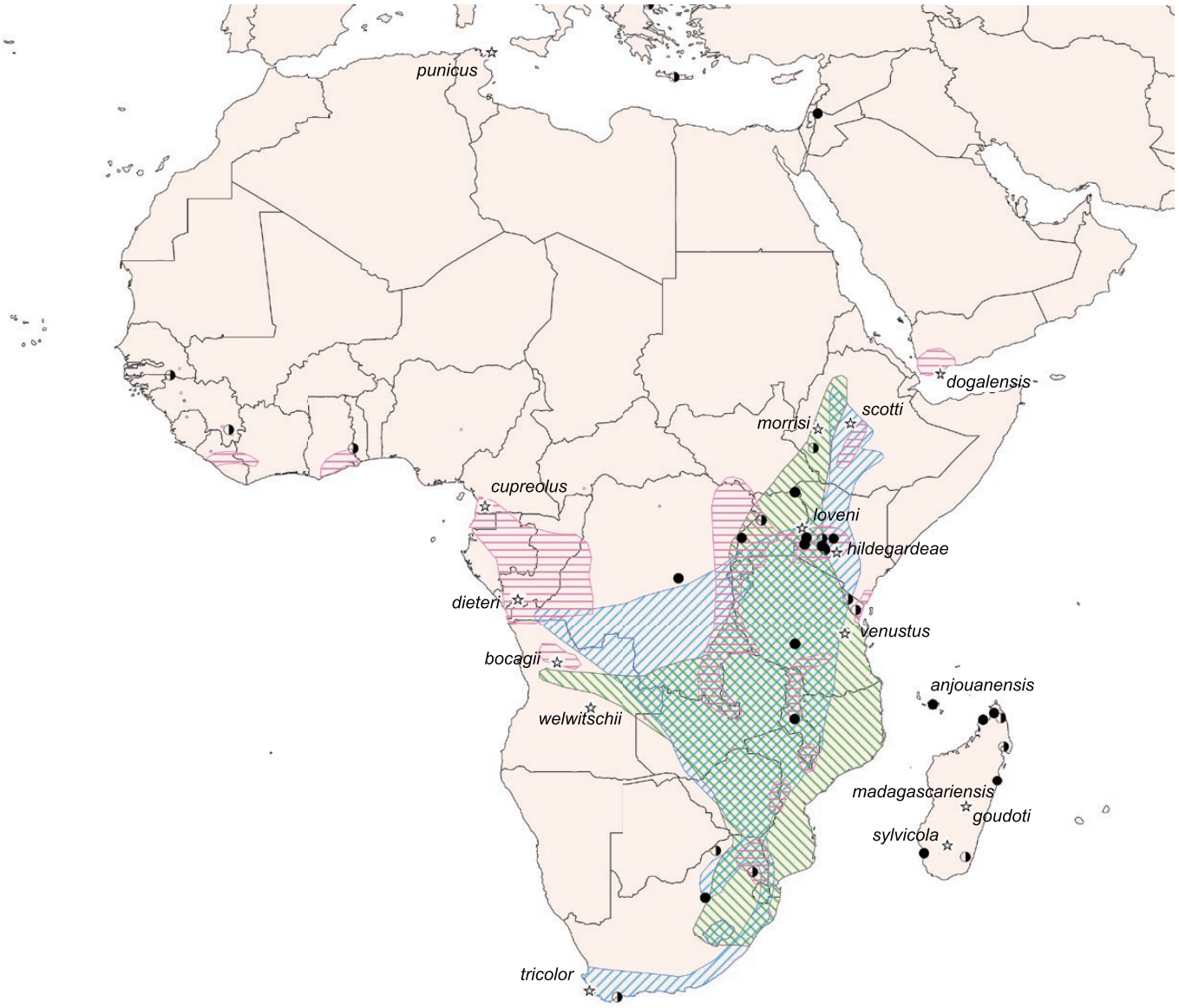

Fig. 1.—Map of Afrotropical *Myotis*, showing the type localities for named taxa (stars), the locations of analyzed genetic samples (*Cytb*-only, half-filled circles; *Cytb* plus introns, closed circles), and the distributions of the three widespread species (*M. bocagii*, horizontal lines; *M. tricolor*, lines inclined right; and *M. welwitschii*, lines inclined left) as mapped by IUCN Red List (Monadjem and Jacobs 2017a; Monadjem and Jacobs 2017b; Monadjem et al. 2017).

prior to their inclusion in coalescent delimitation and species tree analyses. Default parameters were used with the exception of adjusting the haplotype acceptance threshold to 0.70, which has been shown to reduce the number of unresolved genotypes without increasing false positives (Garrick et al. 2010). Input files for PHASE were generated using the SEQPHASE web server (Flot 2010).

Gene trees and haplotype networks.—Nucleotide substitution models for *Cytb* and each nuclear intron were selected using the corrected Akaike information criterion (AICc) on the maximum-likelihood topology estimated independently for each model in jMODELTEST2 (Darriba et al. 2012); the optimal partitioning scheme and nucleotide substitution models for the concatenated intron alignment were inferred in PartitionFinder 2 (Lanfear et al. 2016) according to the AICc under the greedy search algorithm on CIPRES Science Gateway v.3.1 (Miller et al. 2010). Uncorrected sequence divergences (*p*-distances) within and between clades were calculated for *Cytb* in MEGA X 10.0.5 (Kumar et al. 2018). Only a single *Cytb* sequence each was available for *M. anjouanensis* and *M. scotti*, so there can be no estimate of their within-clade variation.

Maximum-likelihood estimates of gene trees for *Cytb*, individual intron alignments, and a concatenated alignment of the four introns were made using the program IQ-TREE version 1.6.0 (Nguyen et al. 2015) on the CIPRES portal. We searched for the best-scoring ML tree algorithm (Hoang et al. 2018) with 1,000 bootstrap and 1,000 topology replicates. Bayesian gene tree analyses for the same alignments were carried out with MRBAYES v.3.2.6 (Ronquist et al. 2012) on the CIPRES portal. Two replicates were run to ensure proper mixing had

occurred. Four Markov chains with default heating values were conducted for 1×10^7 generations and sampled every 1,000th generation. Stationarity was assessed using Tracer v.1.7 (Rambaut et al. 2018). The first 2,500 samples were discarded as burn-in, and the remaining 15,000 samples were used to estimate posterior probability (PP) distributions. Majority-rule consensus trees were generated for each analysis.

Network relationships of *Cytb* for members of the clade containing Afrotropical *Myotis* were assessed in a single analysis of all haplotypes for the following species: *anjouanensis*, *bocagii*, *emarginatus*, *formosus*, *goudoti*, *rufoniger*, *scotti*, *tricolor*, and *welwitschii*. Network analysis was carried out with the median-joining network setting in PopArt version 1.7 (Leigh and Bryant 2015). We also plotted pie charts to visualize the relative frequencies and relationships of alleles in each population.

Coalescent population delimitation and species trees.—We carried out joint multi-locus population delimitation and species tree estimation using the program BPP v.3.3 (Yang and Rannala 2014; Yang 2015). BPP analyses were conducted using well-supported clades common to the mitochondrial and nuclear gene tree analyses. We treated clades within *M. tricolor* and *M. welwitschii* as putatively independent lineages, effectively placing a maximum on the number of lineages that could be delimited by these analyses. BPP is known to be sensitive to effective population size and divergence time priors in relation to delimitation probabilities (Leaché and Fujita 2010; Yang and Rannala 2010). Following the approach of Giarla et al. (2018), we used two replicates for four sets of priors, representing all combinations of deep and shallow divergence depths ($\tau = \Gamma$ [1, 10] and $\tau = \Gamma$ [2, 2000], respectively) and large and small relative mutation-rate-scaled effective population sizes ($\theta = \Gamma$ [1, 10] and $\theta = \Gamma$ [2, 2000]: Prior Set 1 (PS1) $\tau = \Gamma$ [1, 10], $\theta = \Gamma$ [1, 10]; PS2 $\tau = \Gamma$ [2, 2000], $\theta = \Gamma$ [1, 10]; PS3 $\tau = \Gamma$ [2, 2000], $\theta = \Gamma$ [2, 2000]; PS4 $\tau = \Gamma$ [1, 10], $\theta = \Gamma$ [2, 2000]. All BPP analyses were run for 10^5 generations using a burn-in of 10^4 generations and samples recorded every 10th generation. Support for delimitation was assessed where PP ≥ 0.95 indicates strong support for the evolutionary independence of a given population. Our motivation in conducting "species delimitation" analyses was not to explicitly test for species status of populations per se, as the multi-species coalescent cannot statistically distinguish structure associated with population isolation from species boundaries (Sukumaran and Knowles 2017; but see Leaché et al. 2018). Rather, the results from multi-locus coalescent delimitation methods can be viewed as assessments of statistical support for independent evolutionary lineages that in turn require independent integrative taxonomic data (e.g., morphology and distribution) to establish firm species limits. Here, we are assessing the extent to which independent nuclear data support population structure identified in the *Cytb* trees and mitochondrial haplotype network analysis.

As in Demos et al. (2018), results from gene-tree analyses were used to assign populations as "candidate species" for species-tree inference in StarBEAST2 (Ogilvie et al. 2017), an extension of BEAST v.2.5.1 (Bouckaert et al. 2014). Species-tree analyses were carried out using the four phased intron alignments with substitution, clock, and tree models unlinked among loci. All loci were assigned the lognormal relaxed-clock model using a Yule tree prior and linear with constant root population size model. We ran the analysis for 2×10^8 generations in four replicate runs. The first 10% of each run was discarded as burn-in and assembled using LOGCOMBINER v.2.4.7 (Drummond et al. 2012) to produce a maximum clade credibility tree in TREEANNOTATOR v.2.4.7 (Drummond et al. 2012). We used Tracer v.1.7 (Rambaut et al. 2018) to assess convergence and stationarity of model parameters based on ESS values and examination of trace files.

All newly generated sequences were deposited in GenBank with accession numbers MK799655-MK799811 (see also Appendix I). Sequence alignments are available from the authors upon request.

Results

The total number of base pairs (bp) for the alignment of 77 *Cytb* sequences used in MEGA to calculate *p*-distances ranged from 1,040 to 1,140 bp (98.6% complete alignment). This alignment was pruned to 71 unique haplotypes for ML and BI gene-tree analyses. An alignment of 67 in-group *Cytb* sequences was used to generate the median-joining network. The number of bp for the nuclear intron alignments used to infer gene trees, coalescent population delimitation, and species trees were: ACOX2, 363 bp; COPS7A, 567 bp; ROGDI, 444 bp; and STAT5A, 385 bp. A total of 27 individuals were included in the concatenated nuclear intron alignment. The best-fit models of nucleotide substitution for each locus estimated by jMODELTEST2 were: 71-sequence *Cytb* = HKY + G; 27-sequence ACOX2 = HKY + G; 25-sequence COPS7A = HKY + I; 27-sequence ROGDI = HKY; 26-sequence STAT5A = HKY + G. The partitioning scheme and best-fit model of nucleotide substitution for the concatenated intron alignment estimated by PartitionFinder 2 was TIM+G under a single partition including all four introns. Uncorrected mitochondrial *p*-distances for Afrotropical *Myotis* clades in the *Cytb* alignment ranged from 0.037 to 0.170 between clades, whereas within-clade distances evident in our sampling scheme ranged from 0.001 to 0.018 (Table 1).

Mitochondrial analyses.—The Bayesian (BI) and maximum likelihood (ML) phylogenetic estimates recovered very similar topologies. In the *Cytb* gene tree (Fig. 2), all recognized species were strongly supported as monophyletic (i.e., maximum-likelihood bootstrap support [BS] ≥ 70%, Bayesian posterior probability [PP] ≥ 0.95), with the exception of Comoros Islands *M. anjouanensis*, which is well supported as sister to Malagasy *M. goudoti* in the ML tree (BS = 100%) but renders *M. goudoti* paraphyletic in the BI tree. Few of the deeper nodes were well supported. The Afrotropical species were not recovered as monophyletic: *Myotis welwitschii* and East Asian *M. rufoniger* were well supported as sisters (BS = 90%, PP = 1.0), to the exclusion of other African species. There was partial support for the group containing all Afrotropical forms sampled plus Asian

Table 1.—Uncorrected mitochondrial *p*-distances within (bolded numbers on diagonal) and between Afrotropical *Myotis* clades, calculated in MEGA X 10.0.5 (Kumar et al. 2018); Palearctic *M. blythii* is included for reference.

Taxon	1	2	3	4	5	6	7	8	9	10	11
1 *blythii*	**0.055**										
2 *bocagii*	0.168	**0.018**									
3 *emarginatus*	0.139	0.148	**0.005**								
4 *formosus*	0.157	0.168	0.120	**0.003**							
5 *goudoti*	0.167	0.144	0.117	0.133	**0.009**						
6 *rufoniger*	0.167	0.165	0.148	0.164	0.144	**0.006**					
7 *tricolor* 1	0.145	0.157	0.111	0.131	0.128	0.137	**0.002**				
8 *tricolor* 2	0.144	0.157	0.112	0.135	0.127	0.132	0.038	**0.010**			
9 *tricolor* 3	0.147	0.155	0.108	0.130	0.121	0.137	0.037	0.037	**0.001**		
10 *welwitschii* 1	0.170	0.156	0.135	0.168	0.142	0.119	0.144	0.143	0.140	**0.003**	
11 *welwitschii* 2	0.168	0.163	0.131	0.168	0.149	0.126	0.139	0.141	0.142	0.043	**0.007**

M. rufoniger and *M. formosus* and Palearctic *M. emarginatus* (BS = 78%, PP = 0.85).

The *Cytb* phylogeny also showed considerable support (BS ≥ 91%, PP ≥ 0.97) for intraspecific clades within the three widespread Afrotropical *Myotis* species. Two groups were recovered within *M. welwitschii*, corresponding to an equatorial group extending from Guinea into western Kenya and a group found in eastern and southern Africa, from Tanzania to South Africa. Sequences of *Cytb* from the two clades differed by 4.3% (Table 1). Two groups were also resolved within *M. bocagii*, distinguishing a Senegalese specimen from far West Africa from the remainder, including material from Ghana, DRC, Kenya, and Tanzania. *Myotis tricolor* was recovered in three separate groups, two corresponding to South African samples and a third from Kenya. These three clades differed by 3.7–3.8% of their *Cytb* sequences (Table 1).

A haplotype network diagram for the clade containing Afrotropical *Myotis* is shown in Fig. 3; no haplotype is shared among these eight species. Notable here are the substantial number of substitutions separating East African haplotypes for both *M. tricolor* and *M. welwitschii* from South African conspecifics. South African samples were lacking in the *M. bocagii* cluster, which instead shows multiple, closely juxtaposed haplotypes (Fig. 3).

Nuclear intron analyses.—The Bayesian (BI) and maximum likelihood (ML) phylogenetic estimates of the concatenated analysis of introns ACOX2, COPS7A, ROGDI, and STAT5A recovered very similar topologies (Fig. 4). Three of the four Afrotropical species represented by multiple *Cytb* haplotypes were recovered as monophyletic in the nuclear analyses, but *M. goudoti* was rendered paraphyletic by the lone sample of *M. anjouanensis*. Our intron analysis lacked representatives of the Asian taxa *M. formosus* and *M. rufoniger*, but *M. bocagii* and *M. goudoti* + *M. anjouanensis* were robustly recovered as sisters. This clade was then joined to the unresolved couplet of *M. tricolor* and *M. emarginatus*. *Myotis welwitschii* was confidently placed as sister to and outside the remaining Afrotropical species. The concatenated analysis resolved some of the intraspecific clades identified in the mitochondrial analyses. *Myotis tricolor* 1 was strongly supported (BS = 92%, PP = 1.0), and there was strong support for *M. welwitschii* 1 (BS = 81%, PP = 1.0). ML and BI gene trees for individual introns are presented in Supplementary Data SD1.

The species tree generated from a combined analysis of four nuclear introns (Fig. 5) had a similar topology to the concatenated intron analyses. The following relationships were all strongly supported with PP = 1.0: ((*M. anjouanensis* + *M. goudoti*) *M. bocagii*); (*M. tricolor* 1 + *M. tricolor* 3); and (*M. welwitschii* 1 + *M. welwitschii* 2). As in the concatenated intron analyses, *M. welwitschii* is supported as sister to the remaining Afrotropical clades, although the sister clade is less well supported. An additional species tree inferred only with recognized species (i.e., lumping the *M. tricolor* and *M. welwitschii* subclades) had an identical topology and nearly identical nodal support (Supplementary Data SD2).

Population delimitation analyses conducted in BPP provided strong support for the evolutionary independence of *M. tricolor* clades 1 and 3 and *M. emarginatus* (Table 2). All analyses, irrespective of the combinations of divergence date and effective population size priors used, support a two-population model for *M. tricolor* with a posterior probability ≥ 0.99.

Discussion

In contrast to parallel studies of variation in other Afrotropical bats, including the vespertilionid *Scotophilus* (Demos et al. 2018), the rhinolophid *Rhinolophus* (Demos et al. In press-a), and the nycterid *Nycteris* (Demos et al. In press-b), all *Myotis* samples were confidently recovered in clades associated with recognized species. If cryptic diversity is documented by our analysis, it is limited to geographically structured clades within the widespread species *M. tricolor* and *M. welwitschii*. Although our geographic sampling of *Myotis* was limited by tissue availability and excluded large areas of southern and western Africa (Fig. 1), the same sampling limitations generally apply to our analyses of *Scotophilus, Rhinolophus*, and *Nycteris*, in which cryptic diversity is rampant. This suggests that *Myotis* diversity in Africa really is far lower than in Eurasia or the Americas. Presumably, the diversity in Africa of the ecologically similar "pipistrelloid" bats (13 species of *Pipistrellus*, 18 species of *Neoromicia*, and six species of *Hypsugo*; mammaldiversity.org) must preempt some of the insect resources otherwise available to *Myotis*, as these groups generally forage using similar slow-hawking flight and both employ steep frequency-modulated echolocation calls to find their food (various species accounts in Happold and Happold

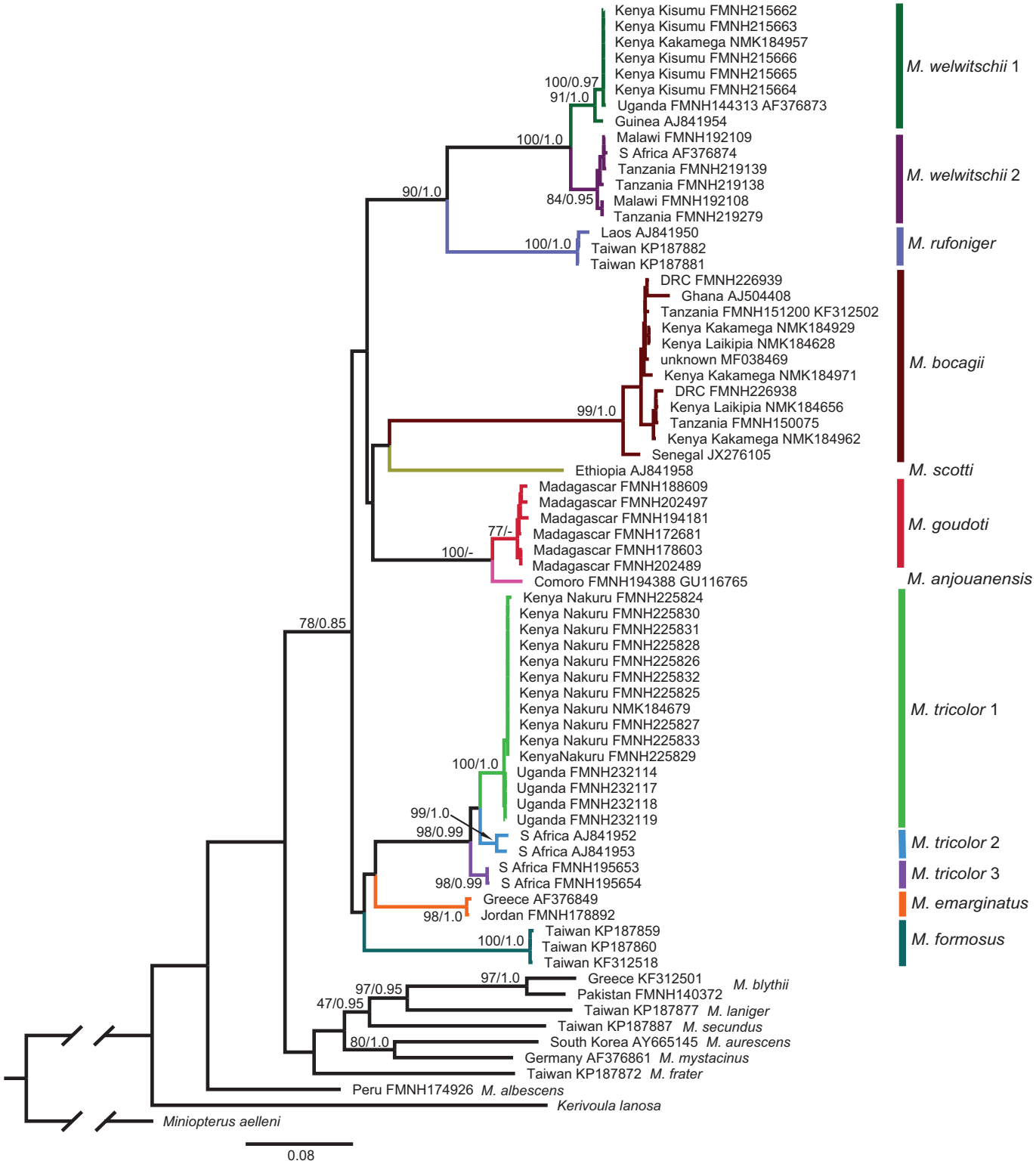

Fig. 2.—Mitochondrial gene tree for Afrotropical *Myotis* inferred using cytochrome-*b*. Paired values at nodes represent bootstrap percentages and posterior probabilities from maximum likelihood and Bayesian analyses, respectively; support values at nodes for most minor clades not shown. Specimen localities include counties for Kenya. Museum acronyms are defined in Appendix I.

2013). Low diversity in Africa does not appear to have a historical explanation: Ruedi et al. (2013) dated the clade containing all known Afrotropical *Myotis* at 12.3 Ma, coincident with the appearance of the New World clade, which now includes 46 species (Larsen et al. 2012; mammaldiversity.org). Our genetic data cannot explain the limited diversity of Afrotropical *Myotis* but they do eliminate a host of unresolved, cryptic lineages as a likely possibility.

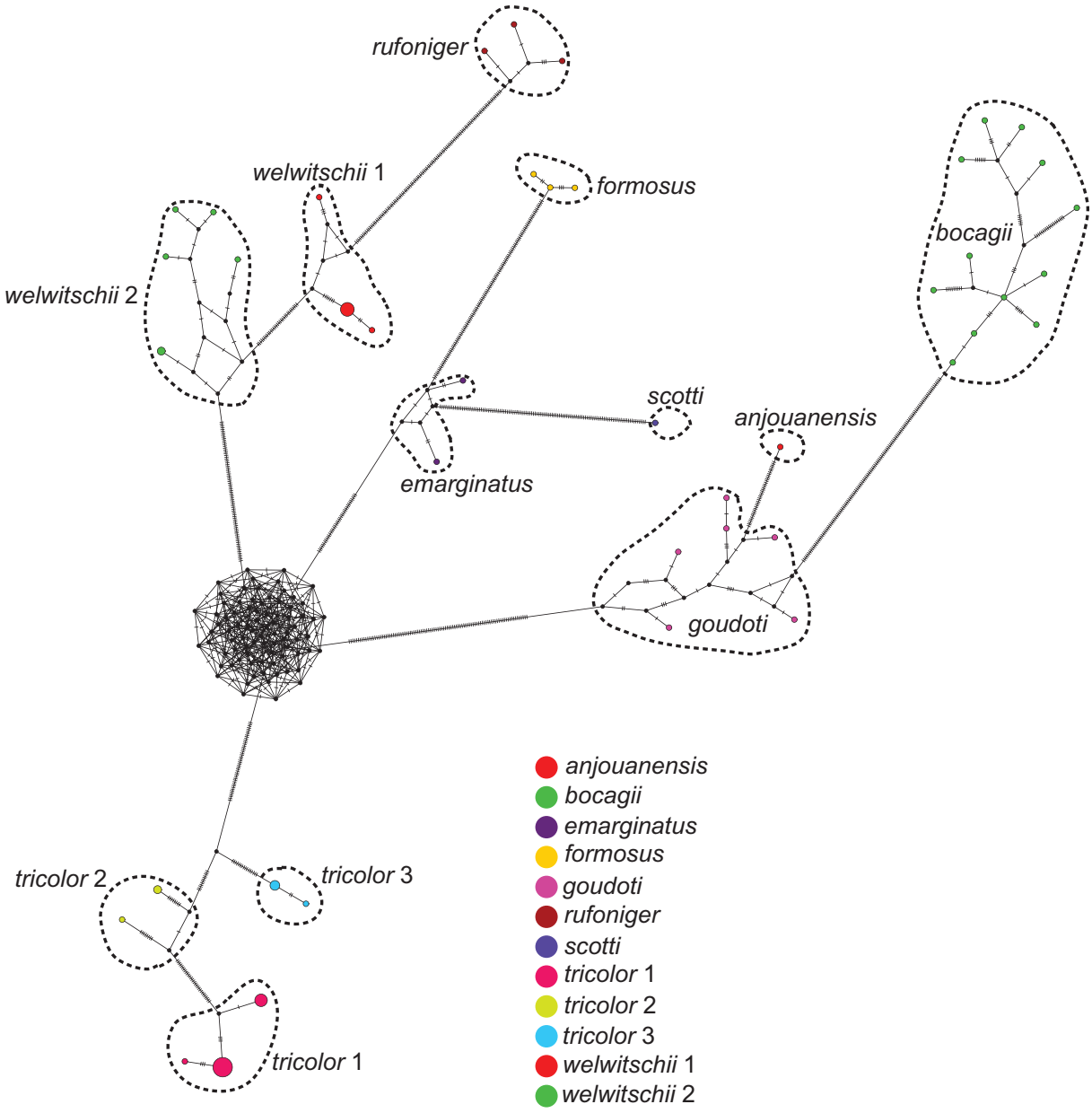

Fig. 3.—PopART network analysis of *Cytb* sequences for the clade containing Afrotropical *Myotis*. Colored circles represent different geographic populations. Black circles represent hypothetical haplotypes connecting those represented by samples. Hatch marks denote base-pair substitutions. See online version for color figure.

Phylogenetic relationships.—Prior phylogenetic reconstructions clearly demonstrated that the Afrotropical (or "Ethiopian") clade of *Myotis* also includes both Palearctic and Indomalayan members; Ruedi and colleagues identified at least *M. emarginatus*, *M. formosus*, and *M. rufoniger* as members of this lineage (Ruedi et al. 2013, 2015). However, the interrelationships of Afrotropical *Myotis* species remained unresolved. Using both *Cytb* and *Rag2*, Ruedi et al. (2013) confidently recovered the group as a whole (*anjouanensis*, *bocagii*, *goudoti*, *scotti*, and *welwitschii*, plus *emarginatus*, *formosus*, and the later-recognized *rufoniger*), and offered strong support for *anjouanensis* + *goudoti* and weak support for *rufoniger* + *welwitschii*; other interspecific nodes for this group were unsupported. Their unsupported topology depicted *tricolor* as sister to all remaining Afrotropical *Myotis*. Using only *Cytb* sequences in a Bayesian analysis, Ruedi et al. (2015) presented a different topology with *M. welwitschii* as sister to the remaining Afrotropical species, but again this topology lacked nodal support.

Our species tree and concatenated intron analyses offer clearer resolution of several previously unresolved nodes. *Myotis bocagii* is confidently recovered as sister to the Indian Ocean clade, here represented by *M. goudoti* + *M. anjouanensis*. This group is strongly recovered as sister to both *M. tricolor* and *M. emarginatus* in the nuclear gene tree, but this relationship has only marginally support in the species tree (PP = 0.90). *Myotis welwitschii* appears strongly supported as the sister to all other sampled members of the Afrotropical

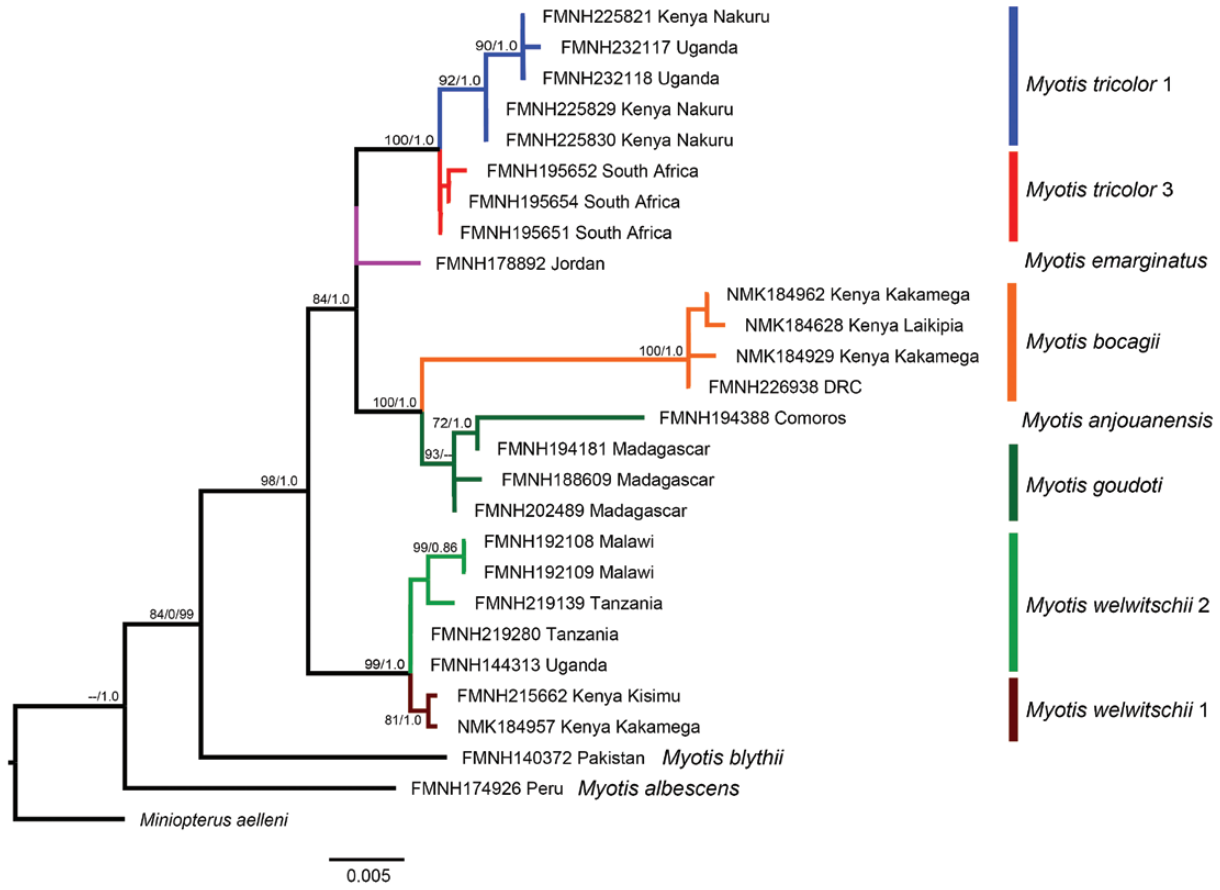

Fig. 4.—Nuclear gene tree for Afrotropical *Myotis* inferred from the concatenation of four introns (ACOX2, COPS7A, ROGDI, and STAT5A). Paired values at nodes represent bootstrap percentages and posterior probabilities from maximum likelihood and Bayesian analyses, respectively; support values at nodes for most minor clades not shown. Specimen localities include counties for Kenya. Museum acronyms are defined in Appendix I.

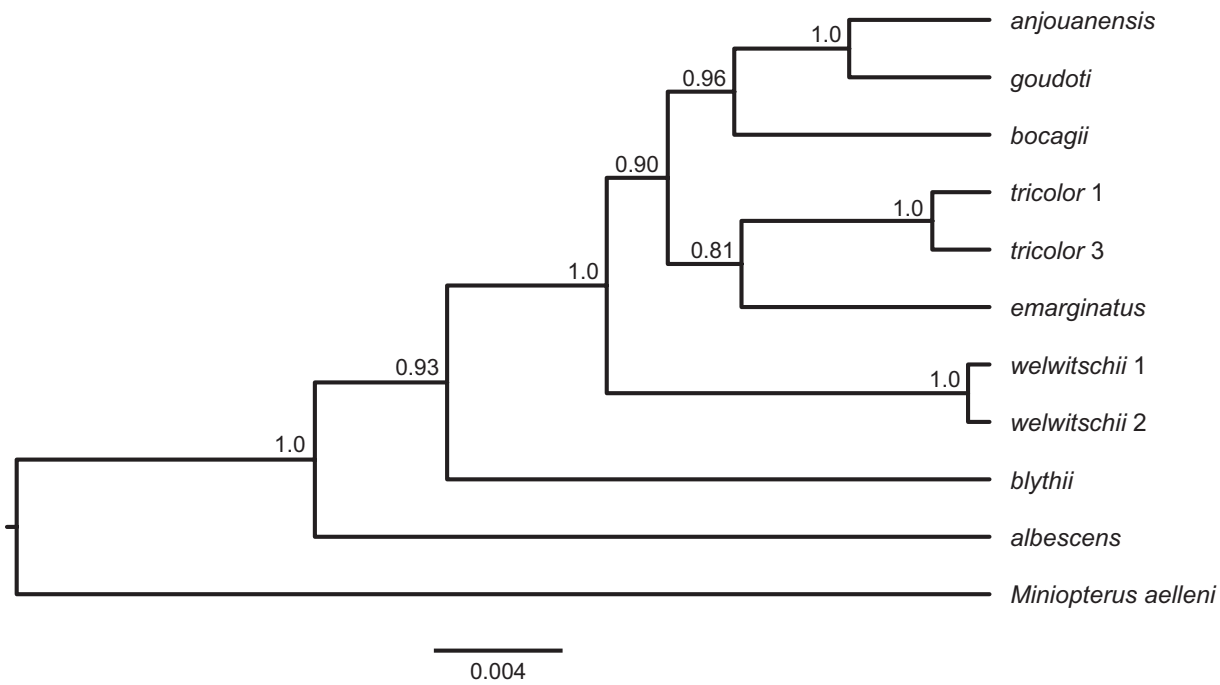

Fig. 5.—Species tree for Afrotropical *Myotis* inferred in StarBEAST2 using four introns (ACOX2, COPS7A, ROGDI, and STAT5A). Numbers at nodes represent posterior probability values.

Table 2.—Lineage delimitation results based on the four intron data set for the Afrotropical clade of *Myotis* under four different parameter sets. See Methods for parameter details.

Putative species	BPP PS1	BPP PS2	BPP PS3	BPP PS4
anjouanensis	0.99	0.99	1.0	1.0
emarginatus	1.0	1.0	1.0	1.0
goudoti	0.99	0.99	1.0	1.0
tricolor clade 1	1.0	1.0	1.0	1.0
tricolor clade 3	1.0	1.0	1.0	1.0
welwitschii clade 1	0.79	0.89	0.96	0.93
welwitschii clade 2	0.79	0.89	0.96	0.93

clade. Although our analysis has many fewer species than the genus-wide analyses of Ruedi et al. (2013, 2015), we employed both Palearctic (*M. blythii*) and Neotropical (*M. albescens*) species to polarize substitutions across four different nuclear loci within the Afrotropical clade.

Evolutionary and taxonomic implications.—Inclusion of *M. dieteri* and *M. morrisi* and more extensive sampling of all taxa are needed to translate our results into a clear understanding of Afrotropical *Myotis*. The lack of *Myotis* samples from many parts of Africa, especially in the west and southwest, makes it likely that some additional species of African *Myotis* remain undiscovered and undescribed. Nevertheless, with reference to Fig. 1, the following observations are possible regarding known species.

Myotis goudoti (A. Smith, 1834) is the only Afrotropical species previously subjected to a molecular phylogeographic analysis. Weyeneth et al. (2011) examined patterns in two mitochondrial genes from sites across Madagascar with very different bioclimatic regimes, finding only modest differentiation but a significant isolation-by-distance effect. Our samples included an individual (FMNH 188609) from Nosy Be, a "landbridge" island 12 km offshore and in 30 m depths that would have been united with Madagascar in the Last Glacial Maximum (Colonna et al. 1996). In keeping with earlier appraisals, mitochondrial variation among all our samples of *M. goudoti* was small (<1%, Table 1), reflecting very recent historical connections. However, nuclear introns of this sample are clearly divergent from Madagascan samples that represent the humid east (FMNH 194181) and arid southwest (FMNH 202489), apparently reflecting reduced gene flow or a founder's effect for this island population (Fig. 4).

Myotis bocagii Peters, 1870 has a type locality of Duque de Bragança, Angola. Two subspecies are currently recognized (Happold 2013a): *M. b. bocagii* in eastern and southern Africa and *M. b. cupreolus* Thomas, 1904 (with a type locality of Efulen, Bulu Country, Cameroon) in central Africa. Two other proposed names are now considered synonyms: *dogalensis* (Monticelli, 1887), from Aden, Yemen, and *hildegardeae* Thomas, 1904, from Fort Hall District, Kenya. Our molecular analysis fails to support the recognition of two subspecies; samples from western Africa (Ghana) and central and eastern Africa (all remaining countries save Senegal and spanning the type locality of *cupreolus*) are strongly united and little divergent in *Cytb* (Fig. 2), and there is no geographic structure to the multiple haplotypes found in this species (Fig. 3). It must be noted that none of our samples actually represent the area where the name *M. bocagii* is based, and Angolan material is needed to confirm its membership in this otherwise cohesive group.

Myotis tricolor (Temminck, 1832) has a type locality of Cape Town, South Africa, and no geographic variation is currently recognized (Bernard 2013), although a single name appears in its synonymy: *loveni* (Granvik, 1924), with type locality on the eastern slopes of Mt. Elgon, Kenya. In contrast with current taxonomy, our mitochondrial analysis documents three substantially divergent clades, separated by 4–5% sequence divergence. One of these is clustered fairly close to Granvik's *loveni* (*tricolor* 1) and the other two are in South Africa (*tricolor* 2 and *tricolor* 3). Concatenated intron analysis shows that *M. tricolor* clades 1 and 3 represent a cohesive, unified entity; still, the coalescent delimitation analyses recover them as significantly distinct evolutionary lineages (Table 1). Integrative taxonomic analysis of morphology and other characters is needed to determine whether the *M. tricolor* haplogroups should be considered clades, subspecies, or even species and whether *tricolor* 1 actually corresponds to Granvik's *loveni*.

Myotis welwitschii (Gray, 1866) has an unspecified type locality in Angola. No subspecies are currently recognized (Happold 2013b), but *venustus* (Matschie, 1899) from Kinole, Ukami Mts, Tanzania is regarded as a synonym. Again with this species, the mitochondrial analyses resolve two reciprocally monophyletic clades, one that is equatorial (western Africa through Uganda to western Kenya) and the other more southern (Tanzania, Malawi, and South Africa). As in *M. tricolor*, these clades differ by 5% in *Cytb* sequence, a level exceeding the differentiation of many well-substantiated bat species (Goodman et al. 2008; Velazco and Patterson 2013; Patterson et al. 2018). These same clades are apparent, but only weakly supported, in the concatenated intron analysis, and appear in only some of the lineage delimitation analyses. Additional geographic sampling is needed to characterize contact between the two forms and to determine 1) which (if either) of the two clades represents typical *welwitschii*, and 2) whether *venustus* applies to the other or is truly a synonym of *welwitschii*.

Many parts of Africa remain unsampled for *Myotis* and these include areas crucial for resolving the group's nomenclature, especially Cape Town, Angola, and western Africa. After morphological analyses, our own samples should provide clear molecular and morphological application of the names *hildegardeae* Thomas, 1904 (for Kenyan *M. bocagii*), *loveni* (Granvik, 1924) (for Kenyan *M. tricolor*), and *venustus* (Matschie, 1899) (for Tanzanian *M. welwitschii*). The western Indian Ocean *Myotis anjouanensis* and *M. goudoti* are well documented and described (Goodman et al. 2010; Weyeneth 2010; Weyeneth et al. 2011). However, Angolan specimens of both *M. bocagii* and *M. welwitschii* are needed to restrict the application of those names to specific clades, and material from Cameroon is needed to better document *cupreolus*. These are obviously vital elements in establishing a definitive nomenclature for the Afrotropical *Myotis*.

Acknowledgments

We thank C. Dick, R. Agwanda, R. Makena, D. Wechuli, R. Yego, and A. Zuhura for help in the field. Our analysis was also strengthened with samples collected by the late W. T. Stanley and M. Abu Baker. The efforts of curators and collection managers in all the institutions cited in Appendix I are acknowledged for maintaining the museum voucher specimens that enable follow-up studies, because these keep our science verifiable and our errors correctable. Field collections in eastern and southern Africa were funded by a variety of agencies in cooperation with the Field Museum, especially the JRS Biodiversity Foundation for support in Kenya. Field Museum's Council on Africa, Marshall Field III Fund, and Barbara E. Brown Fund for Mammal Research were critical to fieldwork and analyses, as was the support of Bud and Onnolee Trapp and Walt and Ellen Newsom. Thanks to the John D. and Catherine T. MacArthur Foundation, Wildlife Conservation Society, Fulbright Program of the U.S. Department of State, and the Centers for Disease Control and Prevention for sponsoring and provision of samples from DRC, Malawi, and Uganda. The Associate Editor and three anonymous reviewers offered criticisms and suggestions that improved the article.

Supplementary Data

Supplementary data are available at *Journal of Mammalogy* online.

Supplementary Data SD1.—Maximum likelihood and Bayesian gene trees for Afrotropical *Myotis*, based on the nuclear introns ACOX2 intron 3 (ACOX2), COPS7A intron 4 (COPS7A), ROGDI intron 7 (ROGDI), and STAT5A intron 16 (STAT5A).

Supplementary Data SD2.—Species tree for recognized species of Afrotropical *Myotis* inferred in StarBEAST2. Numbers at nodes represent posterior probability values. The analysis confirms the same topological relationships with nearly identical support values as in Fig. 5, where both *M. tricolor* and *M. welwitschii* were represented by subclades.

Literature Cited

Bernard, R. T. F. 2013. *Myotis tricolor* Temminck's Myotis (Temminck's Hairy bat). Pp. 706–708 in The Mammals of Africa, Vol 4: Hedgehogs, Shrews and Bats (M. Happold and D. C. D. Happold eds.). Bloomsbury Publishing, London, United Kingdom.

Berthier, P., L. Excoffier, and M. Ruedi. 2006. Recurrent replacement of mtDNA and cryptic hybridization between two sibling bat species *Myotis myotis* and *Myotis blythii*. Proceedings of the Royal Society B: Biological Sciences 273:3101–3109.

Bickham, J. W., J. C. Patton, D. A. Schlitter, I. L. Rautenbach, and R. L. Honeycutt. 2004. Molecular phylogenetics, karyotypic diversity, and partition of the genus *Myotis* (Chiroptera: Vespertilionidae). Molecular Phylogenetics and Evolution 33:333–338.

Bickham, J. W., C. C. Wood, and J. C. Patton. 1995. Biogeographic implications of cytochrome b sequences and allozymes in sockeye (*Oncorhynchus nerka*). The Journal of Heredity 86:140–144.

Bouckaert, R., et al. 2014. BEAST 2: a software platform for Bayesian evolutionary analysis. Plos Computational Biology 10:e1003537.

Colonna, M., J. Casanova, W.-C. Dullo, and G. Camoin. 1996. Sea-level changes and δ18O record for the past 34,000 yr from Mayotte Reef, Indian Ocean. Quaternary Research 46:335–339.

Csorba, G., C. Smeenk, and B. P.-H. Lee. 2016. The identity of *Vespertilio oreias* Temminck, 1840—solving a taxonomic puzzle. Zootaxa 4205:564–570.

Darriba, D., G. L. Taboada, R. Doallo, and D. Posada. 2012. jModelTest 2: more models, new heuristics and parallel computing. Nature Methods 9:772.

Demos, T. C., P. W. Webala, M. Bartonjo, and B. D. Patterson. 2018. Hidden diversity of African Yellow house bats (Vespertilionidae, *Scotophilus*): insights from multilocus phylogenetics and lineage delimitation. Frontiers in Ecology and Evolution 6:86.

Demos, T. C., P. W. Webala, S. M. Goodman, J. C. Kerbis Peterhans, M. Bartonjo, and B. D. Patterson. In press-a. Molecular phylogenetics of the African horseshoe bats (Chiroptera: Rhinolophidae): expanded geographic and taxonomic sampling of the Afrotropics. BMC Evolutionary Biology.

Demos, T. C., P. W. Webala, J. C. Kerbis Peterhans, S. M. Goodman, M. Bartonjo, and B. D. Patterson. In press-b. Molecular phylogenetics of slit-faced bats (Chiroptera: Nycteridae) reveals deeply divergent African lineages. Journal of Zoological Systematics and Evolutionary Research.

Drummond, A. J., M. A. Suchard, D. Xie, and A. Rambaut. 2012. Bayesian phylogenetics with BEAUti and the BEAST 1.7. Molecular Biology and Evolution 29:1969–1973.

Edgar, R. C. 2004. MUSCLE: multiple sequence alignment with high accuracy and high throughput. Nucleic Acids Research 32:1792–1797.

Eick, G. N., D. S. Jacobs, and C. A. Matthee. 2005. A nuclear DNA phylogenetic perspective on the evolution of echolocation and historical biogeography of extant bats (Chiroptera). Molecular Biology and Evolution 22:1869–1886.

Flot, J. F. 2010. Seqphase: a web tool for interconverting phase input/output files and fasta sequence alignments. Molecular Ecology Resources 10:162–166.

Garrick, R. C., P. Sunnucks, and R. J. Dyer. 2010. Nuclear gene phylogeography using PHASE: dealing with unresolved genotypes, lost alleles, and systematic bias in parameter estimation. BMC Evolutionary Biology 10:118.

Ghazali, M., R. Moratelli, and I. Dzeverin. 2017. Ecomorph evolution in *Myotis* (Vespertilionidae, Chiroptera). Journal of Mammalian Evolution 24:475–484.

Giarla, T. C., S. P. Maher, A. S. Achmadi, M. K. Moore, M. T. Swanson, K. C. Rowe, and J. A. Esselstyn. 2018. Isolation by marine barriers and climate explain areas of endemism in an island rodent. Journal of Biogeography 45:2053–2066.

Goodman, S. M., H. M. Bradman, C. P. Maminirina, K. E. Ryan, L. L. Christidis, and B. Appleton. 2008. A new species of *Miniopterus* (Chiroptera: Miniopteridae) from lowland southeastern Madagascar. Mammalian Biology 73:199–213.

Goodman, S. M., N. Weyeneth, Y. Ibrahim, I. Saïd, and M. Ruedi. 2010. A review of the bat fauna of the Comoro Archipelago. Acta Chiropterologica 12:117–141.

Happold, M. 2013a. *Myotis bocagii* Rufous Myotis (Rufous mouse-eared bat). Pp. 692–694 in The Mammals of Africa, Vol 4: Hedgehogs, Shrews and Bats (M. Happold and D. C. D. Happold eds.). Bloomsbury Publishing, London, United Kingdom.

Happold, M. 2013b. *Myotis welwitschii* Welwitsch's Myotis. Pp. 708–710 in The Mammals of Africa, Vol 4: Hedgehogs, Shrews

and Bats (M. Happold and D. C. D. Happold eds.). Bloomsbury Publishing, London, United Kingdom.

Happold, M., and D. C. D. Happold. 2013. The Mammals of Africa, Vol. 4: Hedgehogs, Shrews and Bats. Pp. 541–710, Bloomsbury Publishing, London, United Kingdom.

Hoang, D. T., O. Chernomor, A. von Haeseler, B. Q. Minh, and L. S. Vinh. 2018. UFBoot2: improving the ultrafast bootstrap approximation. Molecular Biology and Evolution 35:518–522.

Kumar, S., G. Stecher, M. Li, C. Knyaz, and K. Tamura. 2018. MEGA X: molecular evolutionary genetics analysis across computing platforms. Molecular Biology and Evolution 35:1547–1549.

Lanfear, R., P. B. Frandsen, A. M. Wright, T. Senfeld, And B. Calcott. 2016. PartitionFinder 2: new methods for selecting partitioned models of evolution for molecular and morphological phylogenetic analyses. Molecular Biology and Evolution 34:772–773.

Larsen, R. J., et al. 2012. Genetic diversity of Neotropical *Myotis* (Chiroptera: Vespertilionidae) with an emphasis on South American species. Plos One 7:e46578.

Leaché, A. D., and M. K. Fujita. 2010. Bayesian species delimitation in West African forest geckos (*Hemidactylus fasciatus*). Proceedings of the Royal Society of London B: Biological Sciences 277:3071–3077.

Leaché, A. D., T. Zhu, B. Rannala, and Z. Yang. 2018. The spectre of too many species. Systematic Biology 68:168–181.

Leigh, J. W., and D. Bryant. 2015. PopART: full-feature software for haplotype network construction. Methods in Ecology and Evolution 6:1110–1116.

Miller, M. A., W. Pfeiffer, and T. Schwartz. 2010. Creating the CIPRES Science Gateway for inference of large phylogenetic trees. Gateway Computing Environments Workshop (GCE). IEEE. doi:10.1109/GCE.2010.5676129, New Orleans, Los Angeles.

Monadjem, A., and D. K. Jacobs. 2017a. *Myotis bocagii*. The IUCN Red List of Threatened Species 2017: e.T14148A22059585.

Monadjem, A., and D. K. Jacobs. 2017b. *Myotis tricolor*. The IUCN Red List of Threatened Species 2017: e.T14207A22063832.

Monadjem, A., P. J. Taylor, D. S. Jacobs, and F. P. D. Cotterill. 2017. *Myotis welwitschii*. The IUCN Red List of Threatened Species 2017: e.T14211A22068792.

Morales, A. E., and B. C. Carstens. 2018. Evidence that *Myotis lucifugus* "subspecies" are five nonsister species, despite gene flow. Systematic Biology 67:756–769.

Nguyen, L. T., H. A. Schmidt, A. von Haeseler, and B. Q. Minh. 2015. IQ-TREE: a fast and effective stochastic algorithm for estimating maximum-likelihood phylogenies. Molecular Biology and Evolution 32:268–274.

Ogilvie, H. A., R. R. Bouckaert, and A. J. Drummond. 2017. StarBEAST2 brings faster species tree inference and accurate estimates of substitution rates. Molecular Biology and Evolution 34:2101–2114.

Patterson, B. D., and P. W. Webala. 2012. Keys to the bats (Mammalia: Chiroptera) of East Africa. Fieldiana: Life and Earth Sciences 6:1–63.

Patterson, B. D., P. W. Webala, M. Bartonjo, J. Nziza, C. W. Dick, and T. C. Demos. 2018. On the taxonomic status and distribution of African species of *Otomops* (Chiroptera: Molossidae). Peerj 6:e4864.

Rambaut, A., A. J. Drummond, D. Xie, G. Baele, and M. A. Suchard. 2018. Posterior summarization in Bayesian phylogenetics using tracer 1.7. Systematic Biology 67:901–904.

Ronquist, F., et al. 2012. MrBayes 3.2: efficient Bayesian phylogenetic inference and model choice across a large model space. Systematic Biology 61:539–542.

Ruedi, M., G. Csorba, L. K. Lin, and C. H. Chou. 2015. Molecular phylogeny and morphological revision of *Myotis* bats (Chiroptera: Vespertilionidae) from Taiwan and adjacent China. Zootaxa 3920:301–342.

Ruedi, M., and F. Mayer. 2001. Molecular systematics of bats of the genus *Myotis* (Vespertilionidae) suggests deterministic ecomorphological convergences. Molecular Phylogenetics and Evolution 21:436–448.

Ruedi, M., B. Stadelmann, Y. Gager, E. J. Douzery, C. M. Francis, L.-K. Lin, A. Guillén-Servent, and A. Cibois. 2013. Molecular phylogenetic reconstructions identify East Asia as the cradle for the evolution of the cosmopolitan genus *Myotis* (Mammalia, Chiroptera). Molecular Phylogenetics and Evolution 69:437–449.

Salicini, I., C. Ibáñez, and J. Juste. 2011. Multilocus phylogeny and species delimitation within the Natterer's bat species complex in the western Palearctic. Molecular Phylogenetics and Evolution 61:888–898.

Sikes, R. S., and The Animal Care and Use Committee of the American Society of Mammalogists. 2016. 2016 Guidelines of the American Society of Mammalogists for the use of wild mammals in research and education. Journal of Mammalogy 97:663–688.

Stadelmann, B., D. S. Jacobs, C. Schoeman, and M. Ruedi. 2004. Phylogeny of African *Myotis* bats (Chiroptera, Vespertilionidae) inferred from cytochrome-b sequences. Acta Chiropterologica 6:177–192.

Stephens, M., N. J. Smith, and P. Donnelly. 2001. A new statistical method for haplotype reconstruction from population data. American Journal of Human Genetics 68:978–989.

Sukumaran, J., and L. L. Knowles. 2017. Multispecies coalescent delimits structure, not species. Proceedings of the National Academy of Sciences of the United States of America 114:1607–1612.

Velazco, P. M., and B. D. Patterson. 2013. Diversification of the yellow-shouldered bats, genus *Sturnira* (Chiroptera, Phyllostomidae), in the New World tropics. Molecular Phylogenetics and Evolution 68:683–698.

Weyeneth, N. 2010. Phylogeography of *Myotis*, *Miniopterus* and *Emballonura* bats from the Comoros and Madagascar. D. Sc., l'Université de Genève, Switzerland.

Weyeneth, N., S. M. Goodman, and M. Ruedi. 2011. Do diversification models of Madagascar's biota explain the population structure of the endemic bat *Myotis goudoti* (Chiroptera: Vespertilionidae)? Journal of Biogeography 38:44–54.

Yang, Z. 2015. The BPP program for species tree estimation and species delimitation. Current Zoology 61:854–865.

Yang, Z., and B. Rannala. 2010. Bayesian species delimitation using multilocus sequence data. Proceedings of the National Academy of Sciences of the United States of America 107:9264–9269.

Yang, Z., and B. Rannala. 2014. Unguided species delimitation using DNA sequence data from multiple loci. Molecular Biology and Evolution 31:3125–3135.

Submitted 28 November 2018. Accepted 24 April 2019.

Associate Editor was Antoinette Piaggio.

Appendix I

List of specimens used in genetic analyses of *Myotis*. Specimen details, localities, and GenBank accession numbers of sampled individuals of *Myotis*: FMNH—Field Museum of Natural History; IVB—Institute of Vertebrate Biology, Academy of Sciences of the Czech Republic, Brno; MHNG—Muséum d'Histoire Naturelle, Geneva; NMK—National Museums of Kenya, Nairobi; NMNS—National Museum of Natural Science, Taichung, Taiwan; OCUMS—Osaka City University; ROM—Royal Ontario Museum, Toronto; TESRI—Taiwan Endemic Species Research Institute, Nantou; THUMB—Biology Department of Tunghai University; TM—Ditsong Museum of Natural History (formerly Transvaal Museum), Pretoria; ZMMU—Zoological Museum of Moscow University.

Institution	Cat. No.	Species	*Cytb*	*ACOX2*	*COPS*	*ROGDI*	*STAT5*	Country	Locality	Latitude	Longitude
FMNH	174926	*Myotis albescens*	MK799657	MK799707	MK799733	MK799757	MK799783	Peru	Maskoitania	−12.7717	−71.3855
FMNH	194388	*Myotis anjouanensis*	GU116765	MK799708	MK799734	MK799758	MK799784	Comoros	Anjouan, Bouelaouvanga	−12.2939	44.4272
none		*Myotis aurascens*	AY665145					South Korea		36.5000	128.0000
FMNH	140372	*Myotis blythii*	MK799658	MK799709	MK799735	MK799759	MK799785	Pakistan	Karakar Pass	34.4333	72.2167
none	MR-583	*Myotis blythii*	KF312501					Greece	Crete	35.2000	24.9000
SMF	89673	*Myotis bocagii*	AJ504408					Ghana	Agmasta wildlife sanctuary	7.1246	0.5914
FMNH	150075	*Myotis bocagii*	MK799666					Tanzania	6 km NW Amani	−5.0667	38.6000
FMNH	226938	*Myotis bocagii*	MK799659	MK799710	MK799736	MK799760	MK799786	Dem. Rep. Congo	Luijo River	−2.6789	25.2252
FMNH	226939	*Myotis bocagii*	MK799660					Dem. Rep. Congo	Luijo River	−2.6789	25.2252
NMK	184929	*Myotis bocagii*	MK799661	MK799711	MK799737	MK799761	MK799787	Kenya	Mungokho Village	0.3749	34.8985
NMK	184962	*Myotis bocagii*	MK799662	MK799712	MK799738	MK799762	MK799788	Kenya	Kakamega Forest, Isiukhu	0.3316	34.8788
NMK	184971	*Myotis bocagii*	MK799663					Kenya	Kakamega Forest, Kisere bridge	0.3958	34.8831
NMK	184628	*Myotis bocagii*	MK799664	MK799713	MK799739	MK799763	MK799789	Kenya	Ol Jogi, Water Treatment Site	0.3040	36.9253
NMK	184656	*Myotis bocagii*	MK799665					Kenya	Ol Jogi, Pyramid Camp	0.3093	36.0761
?	C07-18	*Myotis bocagii*	MF038469								
IVB	S508	*Myotis bocagii*	JX276105					Senegal	Gué de Sambaillou	12.6500	−13.3167
FMNH	151200	*Myotis bocagii*	KF312502					Tanzania	2 km SW Gonja Maore	−4.2667	38.0333
MHNG	1807.04	*Myotis emarginatus*	AF376849					Greece	Thessaloniki, Macedonia	40.6402	22.9629
FMNH	178892	*Myotis emarginatus*	MK799667	MK799714	MK799740	MK799764	MK799790	Jordan	Birqish	32.4333	35.7333
NMNS	t-4607	*Myotis formosus*	KP187859					Taiwan	Heping District, Taichung City	14.5850	107.1350
THUMB	100	*Myotis formosus*	KP187860					Taiwan	Xitun District, Taichung City	23.7200	120.9500
none	MR-590	*Myotis formosus*	KF312518					Taiwan	(lowland)	23.6000	121.2000
TESRI	B0286	*Myotis frater*	KP187872					Taiwan	Wufeng Township	24.6300	121.1191
FMNH	172681	*Myotis goudoti*	MK799668					Madagascar	Antsahabe River, near Ankijabe	−13.2600	49.6350
FMNH	178603	*Myotis goudoti*	MK799669					Madagascar	2.3 km SW Befotaka	−23.8295	46.9683
FMNH	188609	*Myotis goudoti*	MK799670	MK799715	MK799741	MK799765	MK799791	Madagascar	Nosy Be, 1.5 km E Hell-Ville	−13.4067	48.2917
FMNH	194181	*Myotis goudoti*	MK799671	MK799716	MK799742	MK799766	MK799792	Madagascar	Station Forestiere d'Ivoloina	−18.0569	49.3592

APPENDIX I Continued

Institution	Cat. No.	Species	*Cytb*	*ACOX2*	*COPS*	*ROGDI*	*STAT5*	Country	Locality	Latitude	Longitude
FMNH	202489	*Myotis goudoti*	MK799672	MK799717		MK799767		Madagascar	Grotte d'Ambanila,	−23.5400	43.7461
FMNH	202497	*Myotis goudoti*	GU116767					Madagascar	7.5 km SW Mahalevona	−15.4282	49.8453
THUMB	106	*Myotis laniger*	KP187877					Taiwan	Dongshi District, Taichung City	24.2531	120.8576
MHNG	1805.081	*Myotis mystacinus*	AF376861					Germany & Switzerland			
ROM	110544	*Myotis rufoniger*	AJ841950					Laos	Banks of Xe Kaman	14.7537	107.4818
THUMB	30063	*Myotis rufoniger*	KP187882					Taiwan	Yuli Township	23.3723	121.3710
THUMB	30046	*Myotis rufoniger*	KP187881					Taiwan	Alishan Township	23.4363	120.7531
ZMMU	167226	*Myotis scotti*	AJ841958					Ethiopia	Coccia	7.1333	35.4167
TESRI	B0268	*Myotis secundus*	KP187887					Taiwan	Wufeng Township		
TM	40300	*Myotis tricolor*	AJ841952					South Africa	Blyderivierspoot Nature Reserve	−24.9167	30.8167
FMNH	195651	*Myotis tricolor*	MK799682	MK799721	MK799746	MK799771	MK799796	South Africa	2.7 km WNW Venterskroon	−26.8812	27.2441
FMNH	195652	*Myotis tricolor*	MK799683	MK799722	MK799747	MK799772	MK799797	South Africa	2.5 km WNW Venterskroon	−26.8798	27.2454
FMNH	195653	*Myotis tricolor*	MK799684					South Africa	2.5 km WNW Venterskroon	−26.8798	27.2454
FMNH	195654	*Myotis tricolor*	MK799685	MK799723	MK799748	MK799773	MK799798	South Africa	2.5 km WNW Venterskroon	−26.8798	27.2454
FMNH	225821	*Myotis tricolor*	MK799674	MK799718	MK799743	MK799768	MK799793	Kenya	Menengai crater, Mau Mau cave	−0.2516	36.0548
FMNH	225823	*Myotis tricolor*	MK799675					Kenya	Menengai crater, Mau Mau cave	−0.2516	36.0548
FMNH	225824	*Myotis tricolor*	MK799702					Kenya	Menengai crater, Mau Mau cave	−0.2516	36.0548
FMNH	225825	*Myotis tricolor*	MK799676					Kenya	Menengai crater, Mau Mau cave	−0.2516	36.0548
FMNH	225826	*Myotis tricolor*	MK799703					Kenya	Menengai crater, Mau Mau cave	−0.2516	36.0548
FMNH	225827	*Myotis tricolor*	MK799677					Kenya	Menengai crater, Mau Mau cave	−0.2516	36.0548
FMNH	225828	*Myotis tricolor*	MK799704					Kenya	Menengai crater, Mau Mau cave	−0.2516	36.0548
FMNH	225829	*Myotis tricolor*	MK799678	MK799719	MK799744	MK799769	MK799794	Kenya	Menengai crater, Mau Mau cave	−0.2516	36.0548
FMNH	225830	*Myotis tricolor*	MK799705	MK799720	MK799745	MK799770	MK799795	Kenya	Menengai crater, Mau Mau cave	−0.2516	36.0548
FMNH	225831	*Myotis tricolor*	MK799706					Kenya	Menengai crater, Mau Mau cave	−0.2516	36.0548
FMNH	225832	*Myotis tricolor*	MK799679					Kenya	Menengai crater, Mau Mau cave	−0.2516	36.0548
FMNH	225833	*Myotis tricolor*	MK799680					Kenya	Soysambu, Monkey Bridge	−0.3923	36.2112
FMNH	232113	*Myotis tricolor*	MK799686					Uganda	Mt Morungole	3.8108	34.0293
FMNH	232114	*Myotis tricolor*	MK799687					Uganda	Mt Morungole	3.8108	34.0293

APPENDIX I Continued

Institution	Cat. No.	Species	*Cytb*	*ACOX2*	*COPS*	*ROGDI*	*STAT5*	Country	Locality	Latitude	Longitude
FMNH	232117	*Myotis tricolor*	MK799688	MK799724	MK799749	MK799774	MK799799	Uganda	Mt Morungole	3.8108	34.0293
FMNH	232118	*Myotis tricolor*	MK799689	MK799725	MK799750	MK799775	MK799800	Uganda	Mt Morungole	3.8108	34.0293
FMNH	232119	*Myotis tricolor*	MK799690					Uganda	Mt Morungole	3.8108	34.0293
NMK	184679	*Myotis tricolor*	MK799681					Kenya	Gilgil, Pipeline Cave	−0.5391	36.2943
none	—	*Myotis tricolor*	AJ504409					South Africa	Blyderivierspoot Nature Reserve	−24.9167	30.8167
none	—	*Myotis tricolor*	AJ841953					South Africa	De Hoop Nature Reserve	−34.4220	20.5447
TM	39421	*Myotis welwitschii*	AF376874					South Africa	Klipfontein farm 53	−23.3191	28.0438
FMNH	144313	*Myotis welwitschii*	AF376873	MK799732	MK799756	MK799782	MK799807	Uganda	Rwenzori Mts, Mubuku R	0.3500	30.0000
FMNH	192108	*Myotis welwitschii*	MK799697	MK799728	MK799753	MK799778	MK799803	Malawi	Ntchisi Forest Reserve	−13.3797	34.0025
FMNH	192109	*Myotis welwitschii*	MK799698	MK799729	MK799754	MK799779	MK799804	Malawi	Ntchisi Forest Reserve	−13.3797	34.0025
FMNH	215662	*Myotis welwitschii*	MK799692	MK799727	MK799752	MK799777	MK799802	Kenya	Kisimu Impala Sanctuary	−0.1096	34.7459
FMNH	215663	*Myotis welwitschii*	MK799693					Kenya	Kisimu Impala Sanctuary	−0.1096	34.7459
FMNH	215664	*Myotis welwitschii*	MK799694					Kenya	Kisimu Impala Sanctuary	−0.1096	34.7459
FMNH	215665	*Myotis welwitschii*	MK799695					Kenya	Kisimu Impala Sanctuary	−0.1096	34.7459
FMNH	215666	*Myotis welwitschii*	MK799696					Kenya	Kisimu Impala Sanctuary	−0.1096	34.7459
FMNH	219138	*Myotis welwitschii*	MK799699					Tanzania	Ruaha NP, Kilola Star	−7.7071	34.0305
FMNH	219139	*Myotis welwitschii*	MK799700	MK799730	MK799755	MK799780	MK799805	Tanzania	Ruaha NP, Kilola Star	−7.7071	34.0305
FMNH	219279	*Myotis welwitschii*	MK799701					Tanzania	Ruaha NP, Kilola Star	−7.7071	34.0305
FMNH	219280	*Myotis welwitschii*		MK799731		MK799781	MK799806	Tanzania	Ruaha NP, Kilola Star	−7.7071	34.0305
NMK	184957	*Myotis welwitschii*	MK799691	MK799726	MK799751	MK799776	MK799801	Kenya	Kakamega Forest, Buzambuli	0.3501	34.8614
none	JF 105	*Myotis welwitschii*	AJ841954					Guinea	Pic de Fon	8.5333	−8.9000
FMNH	234945	*Kerivoula lanosa*	MK799656					Kenya	Marsabit National Park and Reserve	2.2831	37.9543
FMNH	173067	*Miniopterus aelleni*	MK799655	MK799808	MK799809	MK799810	MK799811	Madagascar	6.2 km NW Mahamasina	−12.9183	49.1267